

Selective NMR Measurements of Homonuclear Scalar Couplings in Isotopically Enriched Solids

Sylvian Cadars,[†] Anne Lesage,[†] Niklas Hedin,[‡] Bradley F. Chmelka,[‡] and Lyndon Emsley^{*,†}

Laboratoire de Chimie (UMR 5182 CNRS/ENS Lyon), Ecole Normale Supérieure de Lyon, Lyon, France, and Department of Chemical Engineering, University of California, Santa Barbara, California 93106

Received: May 12, 2006; In Final Form: June 29, 2006

Scalar (J) couplings in solid-state NMR spectroscopy are sensitive to covalent through-bond interactions that make them informative structural probes for a wide range of complex materials. Until now, however, they have been generally unsuitable for use in isotopically enriched solids, such as proteins or many inorganic solids, because of the complications presented by multiple coupled but nonisolated spins. Such difficulties are overcome by incorporating a z -filter that results in a robust method for measuring pure J -coupling modulations between selected pairs of nuclei in an isotopically enriched spin system. The reliability of the new experimental approach is established by using numerical simulations and tested on fully ^{13}C -labeled polycrystalline L-alanine. It is furthermore shown to be applicable to partially enriched systems, when used in combination with a selective double-quantum (DQ) filter, as demonstrated for the measurement of $^2J(^{29}\text{Si}-\text{O}-^{29}\text{Si})$ couplings in a 50% ^{29}Si -enriched surfactant-templated layered silicate lacking long-range 3D crystallinity. J -coupling constants are obtained with sufficient accuracy to distinguish between different $^{29}\text{Si}-\text{O}-^{29}\text{Si}$ pairs, shedding insight on the local structure of the silicate framework. The new experiment is appropriate for fully or partially enriched liquid or solid samples.

1. Introduction

Scalar (J) couplings have been used in liquid-state NMR since its inception, as central inputs for the determination of complex molecular structures, through the use, for example, of Karplus relationships,¹ which empirically correlate $^3J_{\text{HH}}$ couplings to dihedral angles, for example, or for the determination of atomic connectivities. Even very small couplings, such as those observed for hydrogen bonds in proteins, can be used as structural constraints for the precise determination of the secondary structure of complex biomolecules.² In addition, J couplings are responsible for the modulation of the density matrix that is routinely exploited to provide through-bond coherence transfer,³ which is the basis of a vast number of multidimensional NMR experiments.

In solids, despite pioneering early work,^{4–8} J couplings have been exploited for rigid systems only relatively recently, with the introduction of several robust through-bond correlation techniques.^{9–20} In particular, during the past few years, through-bond mediated correlation techniques, complementarily to through-space methods that use dipolar couplings, have enabled significant advances in the structural investigations of biological solids under magic-angle spinning (MAS).²¹ The measurement of J couplings by spin–echo modulation^{22,23} has also recently become of high interest.^{24–27} Despite their weak intensities compared with typically larger and often dominant anisotropic interactions, J couplings as small as 7 Hz have been measured by spin–echo modulation, yielding insights on systems with hydrogen-bond-mediated $^{15}\text{N}-^{15}\text{N}$ J couplings.²⁴ Such measure-

ments are possible because, under MAS, efficient decoupling techniques lead to transverse dephasing times T_2' that are much longer^{28,29} than the inverse of the apparent line width (T_2^*). As a result, though J couplings are often not resolved in one-dimensional (1D) spectra of solids, J multiplets can be observed in a J -resolved dimension where the often dominant inhomogeneous broadening is refocused.^{15,30} In addition, Duma and co-workers³¹ have recently shown theoretically that, for the case of isolated spins pairs, combined effects of chemical shift anisotropy (CSA) and dipole–dipole couplings surprisingly tend to stabilize J -coupling modulations under MAS. Rather than perturb the J modulation, this leads to robust and reliable measurements of J couplings over a wide range of conditions. Such an approach has recently been used to measure $^1J_{\text{CC}}$ couplings along the retinal chromophore chain in bovine rhodopsin using a series of selectively labeled samples, thus shedding new molecular-level insights on the mechanism of sight and visual response.²⁷

Among key remaining challenges with respect to the use of scalar (J) interactions in solid-state NMR is the measurement of J couplings in multispin systems. Indeed, modulation under the influence of multiple interacting spins is invariably observed in isotopically enriched solids, making the measurement of J couplings among individual spin pairs heretofore difficult or impractical in most cases. This is particularly problematic for increasingly widespread cases where isotopic enrichment is used or required, for example, as in NMR studies of proteins, and given the fact that nonselective isotopic enrichment is typically more straightforward to achieve than site-specific labeling. Here, we demonstrate a new robust technique that is appropriate for either liquid or solid samples and which provides pure J -coupling modulations between selected pairs of nuclei in an isotopically enriched spin system. The reliability of the new

* To whom correspondence should be addressed. E-mail: lyndon.emsley@ens-lyon.fr. Tel: +33 4 72 72 84 86. Fax: +33 4 72 72 88 60.

[†] Ecole Normale Supérieure de Lyon.

[‡] University of California, Santa Barbara.

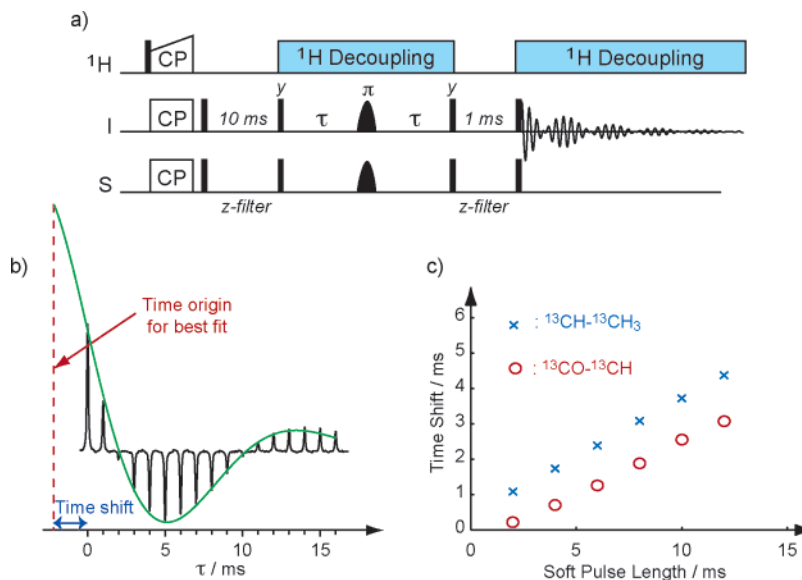


Figure 1. (a) Pulse sequence used for simultaneous refocusing of a selected J -coupled spin pair. I and S correspond to two nuclei of the same type. After the CP step, a first z-filter element is applied to properly define the time origin of the J -coupling modulation (see text for details). A spin-echo period follows, during which a cosine-modulated semiselective pulse is applied to refocus the chemical shift of I and S and undesired J -couplings, while retaining the evolution under J_{IS} . A second z-filter element is finally applied before detection to remove the dispersive anti-phase components of the I -spin magnetization. (b) Experimental behavior of the ^{13}CH resonance of 99% ^{13}C -enriched L-alanine, as a function of the τ delay, observed with the simultaneous refocusing experiment described in (a). A cosine-modulated R-SNOB⁴⁶ pulse of 8 ms duration was used to achieve simultaneous refocusing of the ^{13}CH and ^{13}CO sites. The green line shows the best fit to the experimental peak intensities using a "shifted" cosine function, $\cos(2\pi J(\tau + t_{\text{shift}})) \exp(-2\tau/T_2)$. (c) Fitted time shifts t_{shift} as functions of the length of the refocusing soft pulse. A cosine-modulated Q3⁴⁷ pulse from 2 to 12 ms was used here to achieve simultaneous selective refocusing of J -coupling interactions associated with the $^{13}\text{CH}-^{13}\text{CH}_3$ (blue crosses) or $^{13}\text{CH}-^{13}\text{CO}$ spin pairs (red circles).

experimental approach is established by using numerical simulations and tested on fully ^{13}C -labeled polycrystalline L-alanine. It is furthermore shown to be applicable to partially enriched systems, when used in combination with a selective DQ filter, as demonstrated for the measurement of $^2J(^{29}\text{Si}-\text{O}-^{29}\text{Si})$ couplings in a 50% ^{29}Si -enriched surfactant-templated layered silicate. The measured couplings provide strong additional structural constraints for these technologically important materials, and more generally for the wide range of materials that cannot be characterized by diffusion or diffraction methods because they lack long-range order, and for which solid-state NMR is the only method that provides detailed molecular-level information.

2. Experimental Section

2a. Samples. 99% ^{13}C -enriched polycrystalline L-alanine was used as a model compound to test the new experimental methods introduced here. The sample was obtained from EURISOTOP and used without further purification. $^2J(^{29}\text{Si}-\text{O}-^{29}\text{Si})$ couplings measurements were carried out on a surfactant-templated layered silicate with molecularly ordered 1-nm-thick sheets prepared with 50% ^{29}Si enrichment, as described previously.^{32,33} The development of molecular order and resultant structures of the silicate layers are established by strong interactions between anionic silicate framework moieties and cationic headgroups of the $\text{CH}_3(\text{CH}_2)_{15}-\text{NET}_2\text{Me}^+$ surfactant molecules, which cannot be removed without the collapse and disordering of the layered silicate structure.

2b. ^{13}C NMR Experiments. All experiments were performed on a Bruker AVANCE-500 wide-bore NMR spectrometer operating at ^1H , ^{13}C , and ^{29}Si frequencies of 500.14, 125.76, and 99.35 MHz, respectively. A 2.5-mm CP-MAS probehead, providing MAS sample rotation frequencies up to 35 kHz, was used for the ^{13}C experiments on the 99% ^{13}C -enriched L-alanine.

A 1 ms contact time was used for cross-polarization (CP) from protons to ^{13}C , and proton decoupling was achieved using SPINAL64³⁴ at a nutation frequency of 140 kHz. The spin-echo modulation experiments using the principle of "simultaneous refocusing" were performed by using the pulse sequence shown in Figure 1a, at a MAS frequency of 23 kHz (far from rotational resonance conditions³¹). The τ delay was incremented by multiples of the rotor period (1 ms = $23\tau_R$), and 16 transients were used for each value of τ . The z-filters after CP and before signal acquisition were set to 10 ms and 1 ms, respectively (see explanation below). Simultaneous refocusing was achieved by cosine-modulated shaped pulses, with the frequency of the cosine modulation being half of the desired difference between the two bandwidths. Further specific details are given in the caption of Figure 1.

The z-filtered in-phase anti-phase (IPAP) experiments were acquired at 30 kHz MAS, using the pulse sequence of Figure 2, which was designed as a pseudo-2D experiment, with the τ delay being incremented from 0.8 to 25.6 ms using 0.8 ms increments (24 rotor periods). 32 scans were acquired for each experiment, with a recycle delay of 6 s. Selective refocusing was achieved using 1% truncated Gaussian pulses.³⁵ The z-filters were set to 5 ms after CP and 1 ms before acquisition, respectively. Further specific details are given in the captions of Figure 4.

2c. ^{29}Si NMR Experiments. For the ^{29}Si NMR measurements on the 50% ^{29}Si -enriched surfactant-templated layered silicate, a 4-mm CP-MAS probehead was used at a MAS frequency of 10 kHz, with the temperature of the sample being regulated to 298 ± 1 K. Heteronuclear decoupling was conducted by using the SPINAL64 scheme³⁴ at a proton nutation frequency of 90 kHz. Silicon-29 chemical shifts are referenced to liquid neat TMS (spinning at 2 kHz, with $T = 293$ K). CP from protons to ^{29}Si was achieved using a 9 ms adiabatic passage through the Hartmann-Hahn condition,³⁶ which yields dramatically in-

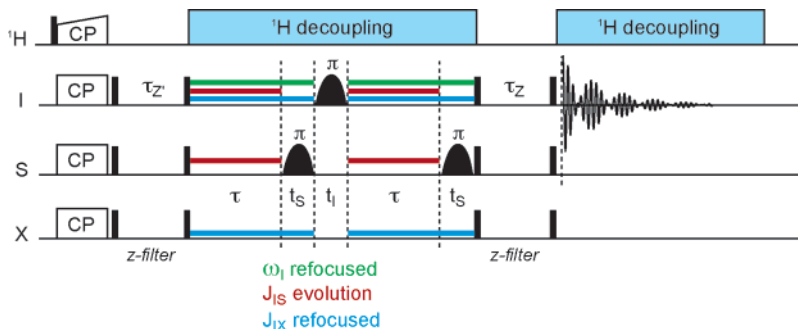


Figure 2. Pulse sequence of the z -filtered IPAP experiment for selective measurement of J couplings in multispin systems. I , S , and X correspond to the same type of nuclei. Two semiselective pulses are applied sequentially in the middle of the echo period, and another one is applied on the S spins at the end of this block. The two selective refocusing pulses on the S spins are identical. As in Figure 1a, z -filter elements are inserted before and after the spin–echo period (see text for details). All of the selective pulses are rotor-synchronized and designed for refocusing (e.g., Gaussian pulses,³⁵ Gaussian cascades,⁴⁷ RE-BURP,³⁷ or R-SNOB⁴⁶).

creased efficiency compared with a ramped CP for this compound, under the conditions used here.

The selective double-quantum (DQ) filtered ^{29}Si experiment was carried out using an experimentally optimized τ_0 delay of 9 ms, with z -filter durations of 500 ms and 13 μs after CP and before acquisition, respectively. Selective excitation of the site 4 spins was achieved using an E-BURP³⁷ shaped excitation pulse of 9.1 ms.

The experiments for measuring $^2J_{\text{SiSi}}$ couplings were acquired according to the pulse sequence of Figure 7a, in similar conditions as those used for the selective DQ-filtered experiment, using E-BURP³⁷ shaped excitation pulses of 9.1 ms and 15 ms for the selective excitation of the Q^4 and the Q^3 ^{29}Si resonances, respectively (because of the smaller isotropic frequency difference between Q^3 sites 1 and 2). The τ_0 delay was set to 9 ms, and τ in the IPAP block was incremented from 2 to 20 or 24 ms (depending on the position of the root of the $\cos(2\pi J\tau)$ function) for the observation of the J modulation. Gaussian pulses³⁵ of 5 ms (Q^4) or 8 ms (Q^3) were used to achieve selective refocusing of both I and S spins. The number of transients ranged between 512 and 2048 (depending on the sensitivity) in the different series of experiments, and the recycle delay was set to 6 to 8 s, which corresponded to an experimental time of 10–50 h for each J -coupling measurement. Long z -filters of 500 ms were used after CP and at the beginning of the z -filtered IPAP block to circumvent probehead heating. The last z -filter, for the removal of anti-phase contributions before acquisition, was set to 50 ms. The estimated errors associated with the J -coupling measurements were calculated by varying randomly the plotted points around the experimental values (according to a Gaussian distribution, whose standard deviation is given by the random noise level) and fitting the obtained curve. This was repeated 4096 times for each set of experiments, yielding a standard deviation of each fitted J value to the experimentally fitted value that was taken as an estimate of the measurement uncertainty.

2d. Numerical Simulations. All simulations results were obtained using the SIMPSON simulation program³⁸ and standard numerical techniques³⁹ on a three-spin system whose parameters correspond to the intramolecular ^{13}C spin system of fully labeled L-alanine. The ^{13}C Larmor frequency was 125.7 MHz. Hard pulses were taken to be “ideal” pulses (i.e., no evolution occurs during the pulse), and soft pulses were implemented as a series of 100 short nonideal pulses, at a radio frequency that was shaped according to a 1% truncated Gaussian envelope. The integrated signal amplitude was obtained from the intensity of the signal of the selected I nucleus. The τ increments were chosen as multiples of the rotor period, as well as the overall

length of the selective pulses. Transverse relaxation was artificially inserted during the processing by using 10-Hz Lorentzian line broadening of the spin–echo evolution. The powder average was performed using a set of 144 $\{\alpha, \beta\}$ angles generated by the REPULSION algorithm⁴⁰ and 12 evenly spaced values of the third Euler angle γ . No significant changes in the integrated signals were observed upon further increase of the number of orientations. MAS frequencies from 6 to 35 kHz were used, and the durations of the soft pulses were varied from 0.5 to 4.0 ms.

3. Selective Measurement of J -Coupling Interactions

3a. Simultaneous Refocusing. There are potentially several ways in which J -coupling measurements might be made selectively in a multispin system. One way is to simultaneously and selectively refocus the scalar interactions experienced by a specific spin pair, according to the sequence of Figure 1a, through the use of cosine-modulated semiselective soft pulses.^{41,42} (Semiselective pulses, which are also referred to as “multiplet-selective pulses”,⁴³ are defined as pulses that irradiate selectively all transitions associated with one multiplet.⁴⁴) Cosine modulation has the effect of splitting the excited region into two bands that are separated by twice the modulation frequency.

In the ideal case of an isolated spin pair in solution, it is well-known that the density matrix at the end of a spin–echo $\tau - \pi_x - \tau$, starting from an initial density matrix $\sigma(0) = -I_y$, is given by

$$\sigma(2\tau) = [I_y \cos(2\pi J_{IS}\tau) - I_x S_z \sin(2\pi J_{IS}\tau)] \exp(-2\tau/T_2) \quad (1)$$

where T_2 is the transverse (liquid-state) relaxation time of the I spins.

However, in the context of simultaneous refocusing of I and S spins by means of a long cosine-modulated soft pulse, the evolution of the in-phase component as a function of τ shows a shift in the position of the zero-crossing, corresponding to the root of the cosine function τ_{root} (which also corresponds to the maximum of the sine-modulated anti-phase coherence), compared with the expected value of $\tau_{\text{root}} = 1/4J$

$$\tau_{\text{root}} = 1/4J - t_{\text{shift}} \quad (2)$$

The time shift t_{shift} arises due to nonnegligible evolution of the simultaneously irradiated J -coupled spins during a long pulse, this evolution being similarly responsible for the creation of undesirable multiple-quantum coherences in the case of semiselective inversion of two J -coupled nuclei, as first shown by Emsley et al.⁴² Using the zero-order average Hamil-

tonian theory, Miao and Freeman⁴⁵ predicted t_{shift} to be

$$t_{\text{shift}} \approx t_p/2 \quad (3)$$

where t_p is the pulse duration, which means that the time origin of the evolution is shifted (backward in time) by half the pulse duration when the two J -coupled spins are simultaneously irradiated. Though this does not predict an intrinsic problem, the authors point out the limited accuracy of the zero-order average Hamiltonian theory used for this prediction, which would require further investigations for accurate determination of the value of τ_{root} in practical cases.

For the case of solids under conditions of MAS, the pulse sequence for simultaneous refocusing of J -coupled spins is shown in Figure 1a. After $^{13}\text{C}\{^1\text{H}\}$ cross-polarization transfer from protons to ^{13}C nuclei, a z -filter (see explanation below) is applied, followed by a rotor-synchronized selective spin-echo (under heteronuclear decoupling) and a second subsequent z -filter for the removal of anti-phase contributions before detection. Figure 1b shows the experimental behavior of the I -spins signal as a function of the τ delay. In the case of an ideal pulse, during which no evolution occurs, the observed magnetization would in most cases reproduce the behavior of an isolated spin pair in solution³¹

$$S(\tau) \propto \exp(2\tau/T_2') \cos(2\pi J\tau) \quad (4)$$

where T_2' is the transverse dephasing time for solids under MAS and heteronuclear decoupling. In practice, because of the long duration of the pulse, the time shift predicted from the liquid-state analysis is clearly visible, as can be seen from the damped cosine fit overlaying the modulated signal intensities in Figure 1b (with a fitted value $t_{\text{shift}} = 2.2$ ms in that particular case.)

For the case of solids under conditions of MAS, the measured shift of the time origin of the modulation, t_{shift} , depends on the duration of the soft pulse applied, as shown in Figure 1c for different J -coupled ^{13}C spin pairs in L-alanine. (This effect is general, and not restricted to the R-SNOB⁴⁶ or Q3⁴⁷ pulse shapes used for parts b and c of Figure 1, though its amplitude might change from one shape to another, for a constant pulse length.) The MAS frequency was chosen such that rotational resonance conditions^{48,49} are avoided. In addition to the linear dependence on the pulse length expected, according to the liquid-state analysis, it can be seen that the behavior of the fitted t_{shift} is significantly different for the $^{13}\text{CH}-^{13}\text{CO}$ or the $^{13}\text{CH}-^{13}\text{CH}_3$ spin pairs. This suggests that there are probably (and not surprisingly) additional effects, due to dipolar couplings and/or CSA interactions, and that the value of the J coupling might also play a role, despite the first-order analysis of eq 3 suggesting that it does not.

The conclusion of Figure 1c is that, unless two roots of the cosine modulation can be precisely observed, simultaneous refocusing of coupled spins using soft pulses is not suitable for quantitative measurements of J couplings. Indeed, only if two roots are present can the time shift be reliably included in the fit procedure. Because this is typically not the case in solid-state NMR, as soon as J couplings are weaker than 20 to 25 Hz, an alternate approach is required.

3b. z -Filtered IPAP. The homonuclear solid-state IPAP sequence was first adapted from a similar heteronuclear liquid-state NMR experiment^{50,51} to detect spin-state-selective spectra in fully enriched solids under conditions of MAS.^{52,53} Interestingly, the homonuclear experiment has since been shown to be useful also in liquids.⁵⁴ In the present paper, the z -filtered IPAP sequence (Figure 2) is used to observe accurately the cosine

modulation that arises from J couplings between a selected pair of spins in a multispin system. The way this sequence works can be understood on the basis of the assumption that, under semiselective irradiation, all of the individual transitions in the selected multiplet evolve as isolated pseudo-spins $I = (1/2)$ (ref 44) (or "fictitious" spins $I = (1/2)$, ref 55) with fictitious chemical shifts, as long as the transitions of the connected spins are not simultaneously irradiated. Moreover, if the pulses that are used are designed for refocusing,^{37,47} then there will be no net evolution under the fictitious chemical shift of the spin and hence no net evolution due to the J couplings during the pulse. Thus, a selective spin-echo sequence must act on each spin in the pair sequentially but still refocus the chemical shifts over the whole period.

In the z -filtered IPAP, CP is immediately followed by a z -filter that properly defines the time origin of the J modulation. Indeed, in view of the discussion above, J -coupling evolution also occurs during CP, since all of the ^{13}C spins are irradiated simultaneously for 1 ms or more. The z -filter is followed by the IPAP block. As shown schematically in green in Figure 2, the chemical shift of spin I is refocused, since it experiences free evolution during $\tau + t_S$, is inverted, and then evolves freely during another $\tau + t_S$ delay. Since no evolution occurs under J_{IS} during pulses on either the I or S spins as long as they are not irradiated simultaneously, the I spins only evolve under J_{IS} during both τ delays (as shown in red in Figure 2). J_{IS} is not refocused, since both spins are refocused between the two τ periods. Finally, the J couplings of the I spins to all other nuclei are refocused, as the I spins are inverted between the two $\tau + t_S$ periods, whereas any other coupled nuclei are not (in blue). The sequence ends with a second z -filter to remove anti-phase contributions to the observed signal, and a pure absorption phase I -spin signal is then detected. (The other spins, on which complicated line shapes are expected, are not considered.) To summarize, we observe a pure cosine modulation of the I spin resonance intensity due to J_{IS} as a function of the τ delay of the echo, while all other J couplings and the chemical shift are refocused.

The results predicted by numerical simulations of a simple J -coupled multispin system with parameters corresponding to the three ^{13}C atoms of fully enriched L-alanine are shown in Figure 3. In Figure 3a, the red plot corresponds to the fitted value of the $^{13}\text{CH}-^{13}\text{CO}$ J coupling from the J modulation, as a function of the MAS spinning frequency. The blue plot represents the standard deviation of the fits. Each pair of blue and red points in these curves corresponds to a fit of the integrated intensity of the I spins, as a function of the τ delay. As long as rotational resonance conditions are avoided (here, $\nu_R = 3.9, 15.8/n$, and $19.7/n$ kHz where $n = 1, 2, 3$, or 4), the fitted J coupling is extremely close to the value used in the simulations (54 Hz for the $^{13}\text{CH}-^{13}\text{CO}$ pair), as shown by the curve in Figure 3b (left), and the agreement between the fit and the simulated data is outstanding. If rotational resonances are matched, then the curve cannot be fitted by a simple cosine-modulation decay since, as can be seen from the central peak in the Fourier transformation of the simulated data in Figure 3c (left), an additional zero-frequency component appears (Figure 3c, right), together with increased noise and stronger dephasing (leading to broader peaks in Figure 3c, right) compared with Figure 3b (right), where the line widths are dominated by the 10 Hz line broadening applied. This effect was previously predicted theoretically and observed experimentally for the case of isolated spin pairs in solids under MAS by Duma et al.³¹ and arises from the combined effects of CSA and dipolar couplings close to rotational resonance. The purpose

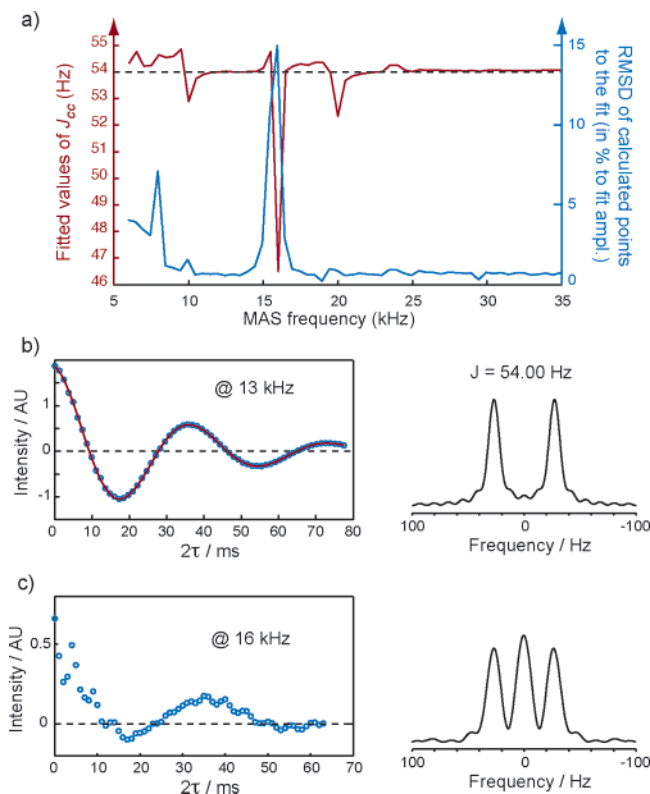


Figure 3. Numerical simulations of the z -filtered IPAP experiment on the ^{13}C spin system of L-alanine. The characteristics of the spin system were chosen as described in ref 71. A magnetic field of 11.74 T was used for the simulations. (a) The red plot shows the fitted value of $^1J(^{13}\text{CO}-^{13}\text{CH})$ as a function of the MAS spinning frequency. Two millisecond Gaussian pulses were used, with I and S corresponding to the ^{13}CH and ^{13}CO carbon spins of L-alanine, respectively. The blue plot shows the root-mean-square deviation (rmsd) of the simulated peak intensities to the best fit, which provides an estimation of the quality of the fit; better fits are thus represented by low rmsd values. (b) (left) Evolution of calculated ^{13}CH peak intensity as a function of the 2τ delay, and corresponding best fit, at a MAS frequency of 13 kHz, which is far from any rotational resonance condition. (right) Fourier transformation of the simulated peak intensities. The τ delay ranged from 0 to about 40 ms, and the plotted intensities correspond to the first point of the free-induction decay of the ^{13}CH resonance. In (c), the same calculations are done at a MAS frequency of 16 kHz, which is close to the $n = 1$ rotational resonance condition for $^{13}\text{CH}-^{13}\text{CO}$ (~ 15.8 kHz).

here is to show that, even in such particular conditions, the behavior observed in multispin systems through the use of the z -filtered IPAP experiment nicely reproduces the behavior of an isolated spin-pair, and the reader is referred to ref 31 for a deeper treatment of the underlying physics.

To test the predictions of the numerical simulations, z -filtered IPAP experiments were carried out on 99% ^{13}C -enriched L-alanine using the pulse sequence of Figure 2. Results are shown in Figure 4, where the integrated intensities of different J -coupled ^{13}C spin pairs are shown for this three-spin system. Figure 4 shows the integrated signal intensities and fits for the ^{13}CH resonance associated with different J -coupled spin pairs, $^{13}\text{CH}-^{13}\text{CH}_3$ and $^{13}\text{CH}-^{13}\text{CO}$, plotted as functions of the delay time τ . As expected, the data are well fitted by single cosine modulations, and the fitted J couplings are found to be very similar to the reference values obtained from z -filtered spin-echo measurements that used a nonselective hard pulse for refocusing and detected the ^{13}CO or $^{13}\text{CH}_3$ resonance (data not shown). Indeed, the fitted value obtained for $^1J(^{13}\text{CH}-^{13}\text{CH}_3)$ is equal to 33.20 ± 0.26 Hz, compared with the 34.25 ± 0.19

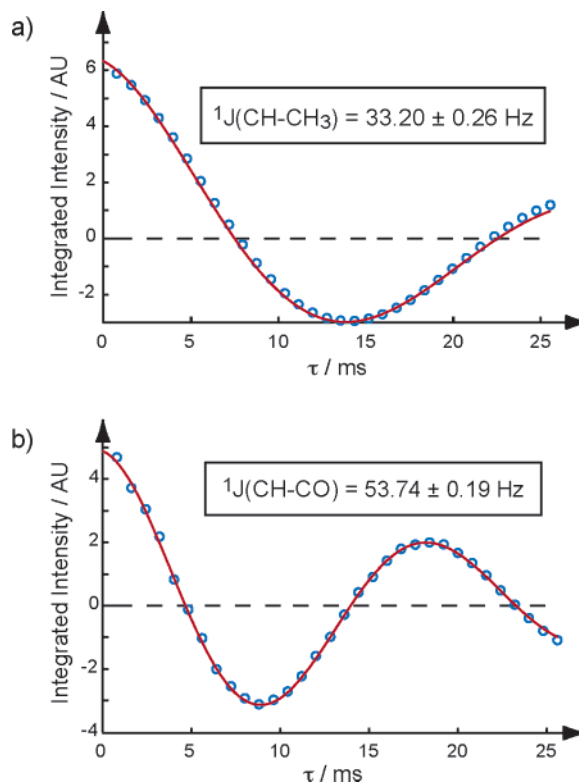


Figure 4. Experimental data obtained using the z -filtered IPAP experiment (Figure 2) on polycrystalline 99% ^{13}C -enriched L-alanine at an MAS spinning frequency of 30 kHz. The experiment was applied, respectively, on the $^{13}\text{CH}-^{13}\text{CH}_3$ (a) and the $^{13}\text{CH}-^{13}\text{CO}$ (b) pairs, with the intensity of the ^{13}CH carbon being detected (i.e., corresponding to the I spins) in both cases. The plotted points correspond to the integrated intensity of the ^{13}CH resonance. Gaussian soft pulses³⁵ of 1 ms (a) and 4 ms (b) were used for refocusing. For each experiment, 512 fits were obtained by adding random noise to the experimental data, with the standard deviation of the noise being twice the standard deviation of the plotted intensities to the fit. The error of the J value was subsequently taken to be the standard deviation of the 512 fitted J values from the value obtained from the experimental data.

Hz value obtained with the nonselective experiment. The agreement is even better for the $^{13}\text{CH}-^{13}\text{CO}$ spin pair for which $^1J(^{13}\text{CH}-^{13}\text{CO})$ was found to be 53.74 ± 0.19 Hz, compared with 53.96 ± 0.25 Hz for the reference experiment. Similar results were obtained by inverting the I and S spins for both pairs, which further demonstrates the reliability of the experiment. Moreover, the experiment was repeated for several soft pulse durations ranging from 1 to 4 ms, and the results were in excellent agreement with the reference values as well. These results demonstrate that the z -filtered IPAP experiment provides an accurate way to measure J couplings in fully enriched multispin systems, independently of the pulse length.

4. Partially Enriched Systems

4a. Limitations Arising from Partial Enrichment. The z -filtered IPAP experiment provides a way to observe selectively single J -coupling modulations in enriched solids. However, systems with only partial enrichment are becoming increasingly widespread, notably in structural studies of proteins and solid-state materials. For such systems, several accommodations must be made to the basic approach outlined above. The problem arises from the fact that an I spin in a partially enriched multispin system may be covalently bonded to either a labeled or a nonlabeled S -type atom, with the probability defined by the level of enrichment. As a consequence, the z -filtered IPAP sequence

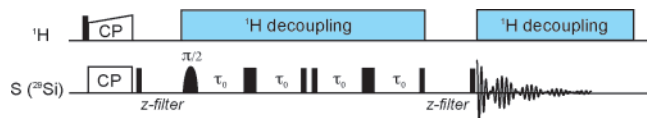


Figure 5. Pulse sequence of the selective through-bond double-quantum filter. After CP, the magnetization is directed back along the z -axis for the desired resonance to be selectively excited. The magnetization of the selectively excited spin is then transferred through homonuclear J couplings to bonded neighbors via a refocused INADEQUATE block. The length of the τ_0 delay is experimentally determined for optimized through-bond transfer.

yields more complex behavior. The signal intensity measured for the I spins as a function of τ is now a superposition of a single-exponential decay weighted by the proportion of unlabeled S -type spins (e.g., ^{12}C , ^{28}Si) and the J_{IS} cosine-modulated exponential decay weighted by the proportion of labeled S -type spins (e.g., ^{13}C , ^{29}Si). Such behavior has previously been observed by Brown et al.²⁶ in 11% ^{13}C -enriched cellulose extracted from wood, using the standard spin-echo experiment for solids. However, in that paper, since a nonselective approach was used, the authors could not distinguish between the couplings due to two potentially enriched neighbors and an average J -coupling constant was given for ^{13}C nuclei that are directly linked to two distinct carbon atoms (the contribution of triply labeled ^{13}C – ^{13}C – ^{13}C fragments being neglected). In the case of large J couplings, long transverse dephasing times T_2' , and good signal-to-noise, where several oscillations of the cosine modulation can be observed, the IPAP sequence can be used directly (with the level of enrichment being additionally determined).

This is the simplest way to extend the analysis proposed in ref 26 to measure “pair-specific” couplings in partially enriched multipins systems. However, in many (if not most) cases, J

couplings of high interest with respect to local structural information will often be much weaker. Usually, only one root of the cosine-modulated component can be observed, because of probehead limitations (such as the duration of high power irradiation) or due to samples with intrinsically short T_2' relaxation times. In these cases, in the presence of unlabeled S -type background moieties, J couplings cannot be determined by using the z -filtered IPAP experiment alone.

4b. Selective DQF- z -IPAP. Nevertheless, the difficulties presented by an otherwise identical non- J -coupled population of spins in a partially enriched solid can be overcome by applying the z -filtered IPAP experiment in combination with a selective double-quantum (DQ) filter (see Figure 5). The selective DQ filter removes the single-exponential contribution to the spin-echo curve by transferring the magnetization from a selected site to its J -coupled neighbors through their shared chemical bonds. This method is based on the refocused INADEQUATE experiment,¹⁵ where a z -filter is inserted after CP to enable the selective excitation of only the desired resonance by using a selective 90° excitation pulse. Only the sites that are J coupled to the excited S spins will yield a signal at the end of this experiment, and these can be selected as discussed previously above and illustrated below. We note that sequences that similarly provide a through-bond mediated magnetization transfer from a selectively excited site in solids have been proposed in the literature and could also have been used here.⁵⁶

4c. Application to Partially ^{29}Si -enriched Layered Silicates.

Recently, the structure of a noncrystalline surfactant-templated silicate with molecularly ordered layers was characterized by Hedin et al., by using a combination of solid-state NMR, X-ray diffraction, and molecular modeling.³³ As shown in Figure 6a,

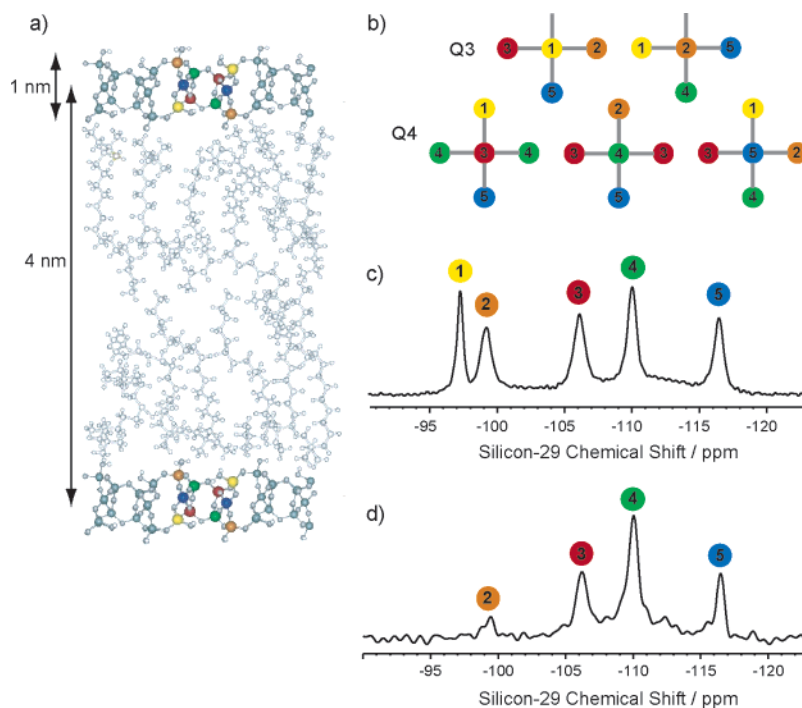


Figure 6. (a) Schematic structure of two surfactant-templated silicate layers, viewed parallel to the layers, which are separated by the alkyl chains of the cationic surfactant species (adapted from Hedin et al.³³). We used the same ^{29}Si site color code to describe the structure of the surfactant-templated silicate sample under investigation in this article. (b) Schematic diagram illustrating ^{29}Si – O – ^{29}Si connectivities among tetrahedrally coordinated Si sites in a surfactant ($\text{C}_{16}\text{–N}^+\text{MeEt}_2$ headgroup)-templated silicate with five molecularly ordered and equally populated Si sites enriched to 50% in ^{29}Si . (c) ^{29}Si CP-MAS spectrum (at 298 K) of the $\text{C}_{16}\text{–N}^+\text{MeEt}_2$ -surfactant-templated silicate layers, acquired within 8 transients, with a recycle delay of 3 s, and a contact time of 9 ms. (d) DQ-filtered ^{29}Si MAS spectrum (at 298 K) of the surfactant-templated silicate material recorded using the pulse sequence of Figure 5. An E-BURP³⁷ soft pulse of 9.1 ms was applied to selectively excite the silicon-29 resonance of site 4. A total of 128 transients were accumulated with a recycle delay of 5 s. The length of the z -filters was set to 15 μs , and the τ_0 delay was 9 ms.

this material is interesting in that it possesses high degrees of both mesoscopic order, established by self-assembly of the surfactant species, as well as local molecular order within its 1-nm-thick silicate sheets, though without the long-range 3D periodicity characteristic of crystalline solids. In these systems, measurement of the ${}^2J({}^{29}\text{Si}-\text{O}-{}^{29}\text{Si})$ couplings is of particular interest, since they are directly related to the geometry of the siloxane linkages. As shown in Figure 6c, for a $\text{CH}_3(\text{CH}_2)_{15}\text{-NEt}_2\text{Me}^+$ -templated silicate sample prepared with 50% ${}^{29}\text{Si}$ enrichment, five well-resolved resonances are observed in the ${}^{29}\text{Si}$ CP-MAS spectrum, consistent with the five distinct, equally populated ${}^{29}\text{Si}$ sites in the material.³² The peaks at -97.3 and -99.3 ppm, labeled sites 1 and 2, respectively, correspond to Q^3 ${}^{29}\text{Si}$ sites, whereas the peaks at -106.1 , -110.0 , and -116.5 ppm (sites 3, 4, and 5, respectively) correspond to fully condensed tetrahedrally coordinated Q^4 ${}^{29}\text{Si}$ sites (where Q^N refers to a Si atom linked to N other Si atoms through siloxane bridges.) The refocused ${}^{29}\text{Si}\{{}^{29}\text{Si}\}$ INADEQUATE¹⁵ spectrum (not shown here) of the material under consideration establishes that the interconnectivities among the five distinct ${}^{29}\text{Si}$ sites are the same as those reported for a related silicate-surfactant material synthesized with a different surfactant headgroup, as described in ref 33: site 1 is linked to sites 2, 3, and 5; site 2 is linked to sites 1, 4, and 5; site 3 to two different site-4 nuclei and once each to sites 1 and 5; site 4 is linked to two different site-3 nuclei and once each to sites 2 and 5; and finally, site 5 is connected to sites 1, 2, 3, and 4. All of these tetrahedral ${}^{29}\text{Si}$ site connectivities are summarized schematically in Figure 6b, where the gray lines correspond to siloxane bridges (and to silanol groups for the Q^3 moieties). The structural analyses of such complicated hierarchically ordered solids have relied on small-angle X-ray scattering to establish the ca. 4-nm spacing between adjacent silicate sheets and a combination of 2D double-quantum ${}^{29}\text{Si}\{{}^{29}\text{Si}\}$ MAS NMR, wide-angle X-ray scattering, and quantum-chemistry calculations to establish local atomic ordering of the 2D silicate frameworks.³³ In the absence of long-range 3D molecular order, NMR is the most informative means of obtaining detailed insights on the local structures of these and similar complex solid materials. As a consequence, every additional constraint that NMR may provide can potentially increase the reliability of the NMR-based structural determination of such solids lacking long-range crystallinity. To that end, the use of the combined double-quantum and z -filtered IPAP experiment to measure ${}^2J({}^{29}\text{Si}-\text{O}-{}^{29}\text{Si})$ couplings are expected to provide strong constraints in the analyses of complicated solid structures, including the surfactant-templated silicates.

4d. Selectively Excited and DQ-filtered Interactions in ${}^{29}\text{Si}$ -enriched Layered Silicates. By selectively exciting a given resonance and then applying a double-quantum filter before detection, it is possible to distinguish the spins that are coupled to the excited nuclei. For example, Figure 6d shows a double-quantum-filtered ${}^{29}\text{Si}$ CP-MAS spectrum obtained using the selective through-bond DQ filter introduced above (with no z -filtered IPAP sequence included), where site 4 has been selectively excited. It can be seen from this DQ-filtered MAS spectrum that the excited site 4 yields the most intense resonance and that magnetization is transferred to sites 2, 3, and 5 but not to site 1. This is consistent with the silicate structure shown in parts a and b of Figure 6, where ${}^{29}\text{Si}$ site 4 is linked via siloxane bridges to sites 2, 3 (twice), and site 5 but not site 1.

Comparison of the conventional CP-MAS and DQ-filtered ${}^{29}\text{Si}$ spectra in parts c and d of Figure 6 for the 50% ${}^{29}\text{Si}$ -enriched layered silicate-surfactant material shows signifi-

cant differences in the intensities of the ${}^{29}\text{Si}$ signals observed. This is due to several factors, including most importantly that only ${}^{29}\text{Si}-\text{O}-{}^{29}\text{Si}$ pairs involving site 4 have been selectively excited and detected. In addition, there is an overall sensitivity loss of about $1/2$ due to the elimination of zero-quantum coherences by the DQ filter, with a portion of the magnetization also lost through transverse dephasing T_2' during the long spin-echoes required due to the weak ${}^{29}\text{Si}-\text{O}-{}^{29}\text{Si}$ J couplings. As expected, in Figure 6d, ${}^{29}\text{Si}$ site 3 yields a signal with significantly greater integrated intensity than sites 2 and 5, consistent with each site 3 being linked to two sites 4 and vice versa. The difference in the ${}^{29}\text{Si}$ signal intensities associated with sites 2 and 5 could be due (i) to differences in CP efficiency from one site to another, (ii) to differences in the J couplings between pairs 2-4, 3-4, and 4-5, since the intensity build up is proportional to $\sin^2(2\pi J_{IS}\tau_0)$ (see Figure 5), and/or (iii) to differences in the T_2' relaxation time from one site to another. At this point, (ii) seems to be the most plausible explanation since, under the conditions used here, the integrated intensities of sites 2 and 5 in the CP-MAS spectrum (Figure 6c) are approximately the same and the effect of the variations of T_2' among the different sites is not expected to be strong (considering the long T_2' values measured in section 5 and the τ_0 delay of 9 ms used here). The efficiency of the DQ filter in the present case, calculated from the intensity of peak 5, is approximately 7% (and less for site 2), and approximately 30% taking into account the level of enrichment (only 25% of the 4-5 pairs are doubly labeled), with the maximum theoretical efficiency being 50% because of the DQ filtering. Better efficiency is expected for larger J couplings, since shorter τ_0 delays can be used in that case, thus reducing the effects of transverse dephasing.

4e. ${}^2J({}^{29}\text{Si}-\text{O}-{}^{29}\text{Si})$ Coupling Measurements in Partially ${}^{29}\text{Si}$ -enriched Layered Silicates. Combining the selective DQ-filtered MAS experiment with the z -filtered IPAP sequence allows ${}^2J({}^{29}\text{Si}-\text{O}-{}^{29}\text{Si})$ measurements of coupled spin pairs to be made with high degrees of selectivity, even in partially enriched multispin systems. Once the ${}^{29}\text{Si}$ magnetization has been selectively transferred through the scalar couplings to the nearest ${}^{29}\text{Si}$ neighbors of the selected S spin (e.g., site 4 in the example of Figure 6c), insertion of the z -filtered IPAP block (Figure 2) permits selective detection of the modulation of magnetization on a spin moiety I produced by J -coupling interactions involving a specific I-S spin pair. In this case, S represents the spins that have been selectively excited at the beginning of the through-bond DQ-filter block, as shown in the pulse sequence of Figure 7a. The I spins to be monitored should be from among the resolved ${}^{29}\text{Si}$ moieties that are covalently bonded via siloxane bridges to the selectively excited S spin moieties.

Two representative examples of quantitative ${}^2J({}^{29}\text{Si}-\text{O}-{}^{29}\text{Si})$ measurements obtained by using the combined DQ-filtered/ z -filtered IPAP (DQ- z -IPAP) experiment are shown in parts b and c of Figure 7 for the noncrystalline lamellar silicate-surfactant mesophase whose molecularly ordered framework is 50% enriched in ${}^{29}\text{Si}$. The experimental points correspond to the integrated signal intensities of the ${}^{29}\text{Si}$ I -spin site of interest, and the error bars correspond to the standard deviation calculated from the noise regions in the spectrum. In both cases (parts b and c of Figure 7), there is no systematic error detectable for the fits, and the same was true for all measurements made. This suggests that random noise appears to be the only significant source of errors in the data. All the results obtained are summarized in Table 1, where it can be seen that ${}^2J_{\text{SiSi}}$ coupling constants were obtained for four of the eight types

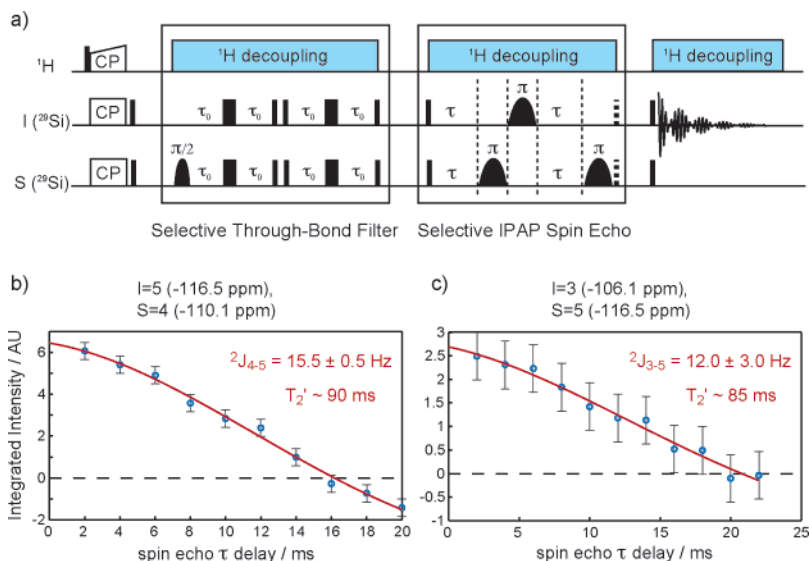


Figure 7. (a) Pulse sequence of the DQ-filtered and z -filtered IPAP (DQ- z -IPAP) experiment. (b) Evolution of integrated peak intensity of site 5 as a function of the τ delay and corresponding fit to a pure cosine-modulated function. The data were obtained by applying the pulse sequence described in (a) with I and S spins corresponding to sites 5 and 4, respectively. (c) Evolution of integrated peak intensity of site 5 as a function of the τ delay and corresponding fit, with I and S spins corresponding to sites 5 and 3, respectively. The fitted values for the two-bond J coupling between the two silicon sites are indicated together with the refocused transverse dephasing time. The spinning frequency was 10 kHz, and SPINAL64³⁴ heteronuclear decoupling at a proton nutation frequency of about 90 kHz was applied. Other experimental details are given in the Experimental Section.

TABLE 1: Experimental ^{29}Si – ^{29}Si J -Coupling Constants Selectively Measured for Four Tetrahedral-site Pairs in a 50% ^{29}Si -enriched Surfactant ($\text{C}_{16}\text{-N}^+\text{MeEt}_2$)-templated Silicate with a Molecularly Ordered Framework

^{29}Si – ^{29}Si spin pair	detected ^{29}Si spin, I	excited ^{29}Si spin, S	${}^2J_{\text{SiSi}}$ (Hz)	T_2' (ms) ^a
4–5	4	5	15.6 ± 0.8	55
	5	4	15.5 ± 0.5	90
3–5	3	5	12.0 ± 3.0	85
	5	3	11.9 ± 1.0	100
2–5	2	5	11.3 ± 0.6	85
1–5			nonmeasurable	
3–4			nonmeasurable	
2–4	2	4	8.2 ± 2.6	70
1–3	1	3	<8	
1–2			nonmeasurable	

^a The T_2' values are estimates, with uncertainties of ca. ± 40 ms, due to signal-to-noise limitations and the limited range of 2τ values used (from 2 to 48 ms).

of ^{29}Si – ^{29}Si linkages in the 50% ^{29}Si -enriched surfactant-templated silicate sample. For the (4–5) and (3–5) ^{29}Si spin pairs shown, the J couplings were separately measured in two different experiments by inverting the sites corresponding to the I and S spin moieties, and in these cases, both values were in excellent agreement, adding further confidence to the results.

Among the ^{29}Si – ^{29}Si spin-site pairs listed in Table 1, several are missing for different reasons that are detailed here (ignoring pairs 1–4 and 2–3 for which covalent linkages do not exist in this sample). First, since each site-4 ^{29}Si is coupled to two site-3 nuclei, and each site 3 to two site-4 ^{29}Si nuclei, it is not possible to observe a single cosine modulation for pair 3–4. Indeed, if site 3 is the selectively excited ^{29}Si site and site 4 is the detected ^{29}Si moiety, the magnetization on site 4 comes from a ^{29}Si -labeled site 3, but site 4 is also coupled to another site 3 that has 50% probability to be nonlabeled. The consequence is a superposition of a single-cosine and a cosine-square modulation under J_{3-4} that interferes with observations of the root of the cosine modulation and makes the measurement of J_{3-4} unfeasible. Second, no root could be observed for the

^{29}Si – ^{29}Si spin pair involving sites 1 and 5, which in this case was probably due to a short T_2' for site 1. For the 1–3 ^{29}Si – ^{29}Si spin pair, which yields very weak intensity correlations in the refocused $^{29}\text{Si}\{^{29}\text{Si}\}$ INADEQUATE spectrum (not shown) compared with the other pairs, the absence of observed zero crossing indicates a J_{1-3} -coupling value that is significantly less than 8 Hz. Finally, the only remaining ^{29}Si spin pair involves sites 1 and 2, which cannot be accessed because of the small difference between the isotropic frequencies of these two peaks (ca. 200 Hz). Such closely spaced isotropic frequencies would require that all of the soft pulses be very long (8 ms for each 180° pulse and about 15 ms for the 90° pulse on the S spins), whereas for ^{29}Si – ^{29}Si pairs 2–4 and 2–5, for which only the I spins (site 2) required such long soft pulses, experimental conditions were already near the limit of feasible probehead high-power-decoupling tolerances.

More generally, the small differences in isotropic frequency among the different resolved resonances (from 200 to 700 Hz at 11.7 T) require the use of long selective pulses, during which high-power proton decoupling must be applied. These limitations, in addition to the long τ_0 delays required for coherence transfer through small ${}^2J_{\text{SiSi}}$ couplings and the long contact time used for CP, lead to particularly long high-power irradiation periods. As a result, to prevent probehead damage, long z -filters (500 ms each) without heteronuclear decoupling were applied after CP and between the DQ filter and the IPAP block and an additional shorter z -filter (50 ms) was inserted before acquisition. ^{29}Si spin-diffusion experiments (see the Supporting Information), acquired under identical MAS and temperature conditions as the J -coupling measurements, show that no (or at least negligible) ^{29}Si – ^{29}Si magnetization transfer through spin diffusion occurs during such z -filters.

Significant quantitative differences are thus observed for the ${}^2J(^{29}\text{Si}$ – $^{29}\text{Si})$ couplings measured selectively for different pairs of ^{29}Si sites in the partially enriched silicate framework of the surfactant-templated solid. In analyzing the results, the ^{29}Si J -coupling values measured appear to depend on the extent of silica site condensation (Q^N) of the nuclei in the spin pair

considered. As shown in Table 1, spin pairs that include Q^3 ^{29}Si sites tend to have J couplings that are smaller (e.g., ${}^2J_{2-4} \sim 8$ Hz and ${}^2J_{1-3} < 8$ Hz) than spin pairs involving two Q^4 moieties. It has been suggested that the proximities and electronegativities of associating ligands may play a role in determining J couplings,^{57,58} which in the present system would be expected to include strongly interacting solvent molecules or ionic species and their accompanying dynamics. Indeed, the cationic surfactant headgroups interact more strongly with anionic Q^3 sites (also H^+ ions associated with silanol moieties) than to more condensed Q^4 sites.

Previous observations of Harris and co-workers in the characterization of aqueous ^{29}Si -enriched silicate anions in liquid-state ^{29}Si NMR measurements reported no clear correlation between ^{29}Si J couplings and the extent of silicate site condensation.⁵⁹ The ${}^2J(^{29}\text{Si}-\text{O}-^{29}\text{Si})$ -coupling values reported in the literature for silicate anions in solution, which range between 3.6 and 10.2 Hz,⁶⁰⁻⁶⁶ are significantly smaller than the values obtained here (except for ${}^2J_{2-4}$, ${}^2J_{1-5}$, and ${}^2J_{2-3}$), which may be due to solvent or internal motions effects. Renewed interest has very recently emerged for the characterization of silicate anions in solution,^{67,68} and new structures have been proposed with the help of quantum-mechanical methods. The ${}^2J_{\text{SiSi}}$ scalar coupling constants reported in refs 67 and 68 (and the values and structures reported by Harris and co-workers^{59,61}) are expected to be useful as a database for establishing J -coupling constant trends, as functions of the local structure, either empirically or by using ab initio J -coupling calculations, since significant progress has been made in these areas (see refs 69 and 70 for reviews).

Nevertheless, in solids, variations in the local geometries of relatively static Si-O-Si framework fragments and ligands, especially Si-O-Si bond angles and Si-Si distances, are expected to dominate the variation in ^{29}Si J couplings between different sites. As mentioned above, a structure was proposed³³ for the molecularly ordered framework of a closely related surfactant-silicate solid, which was synthesized by the cationic surfactant $\text{CH}_3(\text{CH}_2)_{15}-\text{NMe}_2\text{Et}^+$, instead of $\text{CH}_3(\text{CH}_2)_{15}-\text{NEt}_2\text{Me}^+$, for the material studied here. From single-pulse ^{29}Si MAS spectra, both materials have five equally populated, tetrahedrally coordinated Si sites, though with different isotropic ^{29}Si chemical shifts, despite identical X-ray diffraction patterns and $^{29}\text{Si}-\text{O}-^{29}\text{Si}$ site connectivities among the different sites. Taking the layered silicate structures therefore to be similar (within the uncertainties of structures calculated from energy minimization calculations), the J -coupling constants measured here can be plotted as functions of $^{29}\text{Si}-\text{O}-^{29}\text{Si}$ bond angles and distances, as shown in Figure 8. Though the potential error bars are relatively large for the pairs involving a Q^3 site, a qualitative trend is suggested, where larger ${}^2J(^{29}\text{Si}-\text{O}-^{29}\text{Si})$ couplings correspond to larger Si-O-Si bond angles and larger Si-O-Si distances. Further investigations will be required to test the general utility of ${}^2J(^{29}\text{Si}-\text{O}-^{29}\text{Si})$ -coupling data as inputs for the structural determination of crystalline solids and especially materials lacking long-range 3D order, such as proteins or the layered silicates considered here.

5. Conclusions

In summary, the combined selective DQ-filter and z -filtered IPAP experiment allows homonuclear J couplings as small as 8 Hz to be selectively measured in fully and partially enriched multispin systems. The z -filtered IPAP experiment, adapted from solid-state approaches for homonuclear spin-state selection,^{52,53} can be used to measure accurately homonuclear J couplings in

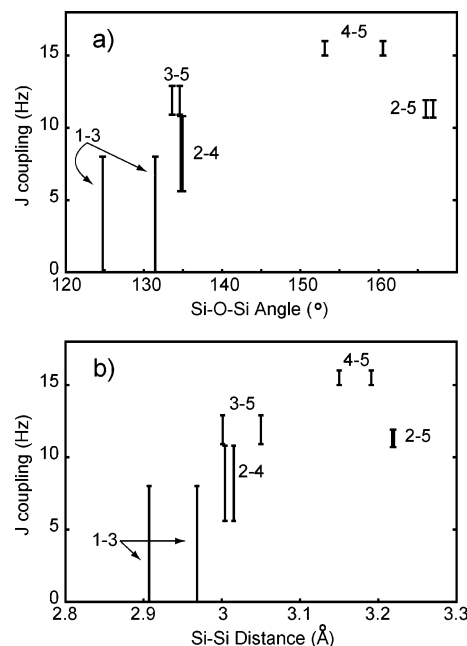


Figure 8. Measured ${}^2J(^{29}\text{Si}-\text{O}-^{29}\text{Si})$ -coupling constants as functions of Si-O-Si bond angles (a) and Si-Si distances (b), assuming that the silicate layers have the same structure as those determined in ref 33 for a closely related system (see text). Error bars between 0 and 8 Hz are used for the 1-3 pair, whose corresponding ${}^2J_{\text{SiSi}}$ -coupling constant is estimated below 8 Hz. Each pair gives rise to two distinct angles and distances, because every site is the superposition of two slightly nonequivalent sites (not resolved in the NMR spectrum) in the structure proposed in ref 33.

fully isotopically enriched solids. In simulations, as well as experimentally, the J modulation obtained with the z -filtered IPAP sequence for fully labeled multispin systems, such as polycrystalline ^{13}C -enriched L-alanine, reproduces accurately the behavior obtained using a standard spin-echo experiment for the ideal case of an isolated two-spin pair, provided rotational resonances are avoided. In partially enriched systems, combining the z -filtered IPAP experiment with a selective double-quantum filter enables the removal of single-exponential decays associated with signals from spins with unlabeled neighbors.

For a fundamentally interesting and technologically important noncrystalline surfactant-templated layered silicate enriched to 50% in ^{29}Si , ${}^2J(^{29}\text{Si}-\text{O}-^{29}\text{Si})$ couplings were obtained for most of the Si-O-Si pairs, ranging from 8.2 to 15.5 Hz, with good accuracy. The significant differences observed in the ${}^2J_{\text{SiSi}}$ coupling constants were attributed to correlations with Si-O-Si bond angles and distances. The approaches presented here for measuring J couplings selectively in isotopically enriched systems (and systems containing naturally abundant spins ($1/2$), such as ^{31}P) are applicable generally to both liquids and solids. Such methodological advancements are anticipated to enable new and accurate measurements of $^{13}\text{C}-^{13}\text{C}$ scalar couplings in partially enriched proteins, ${}^2J_{\text{SiSi}}$ couplings in zeolite molecular sieves or clay minerals, or other multiple-quantum-filtered couplings (e.g., ${}^3J_{\text{CC}}$), from which new and detailed structural and functional insights on the properties of these complicated heterogeneous systems are expected to arise.

Acknowledgment. The authors thank Dr. Almut Rapp and Dr. Jan Dirk Epping for helpful discussions. This work was supported in part by the U.S. National Science Foundation Division of Materials Research under Award DMR-02-33728 and by the USARO through the UCSB Institute for Collaborative Biotechnologies.

Supporting Information Available: Phosphorus-31 spin diffusion spectrum. This material is available free of charge via the Internet at <http://pubs.acs.org>.

References and Notes

- (1) Karplus, M. *J. Am. Chem. Soc.* **1963**, *85*, 2870–2871.
- (2) Grzesiek, S.; Cordier, F.; Jaravine, V.; Barfield, M. *Prog. Nucl. Magn. Reson. Spectrosc.* **2004**, *45*, 275–300.
- (3) Ernst, R. R.; Bodenhausen, G.; Wokaun, A. *Principles of Nuclear Magnetic Resonance in One and Two Dimensions*; Oxford Science Publications: New York, 1987.
- (4) Early, T. A.; John, B. K.; Johnson, L. F. *J. Magn. Reson.* **1987**, *75*, 134–138.
- (5) Benn, R.; Grondey, H.; Brevard, C.; Pagelot, A. *J. Chem. Soc., Chem. Commun.* **1988**, 102–103.
- (6) Fyfe, C. A.; Gies, H.; Feng, Y.; Kokotailo, G. T. *Nature* **1989**, *341*, 223–225.
- (7) Fyfe, C. A.; Gies, H.; Feng, Y. *J. Chem. Soc., Chem. Commun.* **1989**, 1240–1242.
- (8) Gay, I. D.; Jones, C. H. W.; Sharma, R. D. *J. Magn. Reson.* **1991**, *91*, 186–189.
- (9) Baldus, M.; Meier, B. H. *J. Magn. Reson. Ser. A* **1996**, *121*, 65–69.
- (10) Baldus, M.; Iulicci, R. J.; Meier, B. H. *J. Am. Chem. Soc.* **1997**, *119*, 1121–1124.
- (11) Lesage, A.; Auger, C.; Caldarelli, S.; Emsley, L. *J. Am. Chem. Soc.* **1997**, *119*, 7867–7868.
- (12) Lesage, A.; Steuernagel, S.; Emsley, L. *J. Am. Chem. Soc.* **1998**, *120*, 7095–7100.
- (13) Lesage, A.; Sakellariou, D.; Steuernagel, S.; Emsley, L. *J. Am. Chem. Soc.* **1998**, *120*, 13194–13201.
- (14) Verel, R.; van Beek, J. D.; Meier, B. H. *J. Magn. Reson.* **1999**, *140*, 300–303.
- (15) Lesage, A.; Bardet, M.; Emsley, L. *J. Am. Chem. Soc.* **1999**, *121*, 10987–10993.
- (16) Heindrichs, A. S. D.; Geen, H.; Giordani, C.; Titman, J. J. *Chem. Phys. Lett.* **2001**, *335*, 89–96.
- (17) Mueller, L. J.; Elliott, D. W.; Kim, K. C.; Reed, C. A.; Boyd, P. D. W. *J. Am. Chem. Soc.* **2002**, *124*, 9360–9361.
- (18) Sakellariou, D.; Emsley, L. *Encyclopaedia of NMR*; Grant, D. M., Harris, R. K., Eds.; Wiley: London, 2002; Vol. 9, pp 196–211.
- (19) Hardy, E. H.; Detken, A.; Meier, B. H. *J. Magn. Reson.* **2003**, *165*, 208–218.
- (20) Mueller, L. J.; Elliott, D. W.; Leskowitz, G. M.; Struppe, J.; Olsen, R. A.; Kim, K. C.; Reed, C. A. *J. Magn. Reson.* **2004**, *168*, 327–335.
- (21) Ramamoorthy, A. *NMR Spectroscopy in Biological Solids*; CRC Press: Boca Raton, FL, 2005.
- (22) Kubo, A.; McDowell, C. A. *J. Chem. Phys.* **1990**, *92*, 7156–7170.
- (23) Wu, G.; Wasylishen, R. E. *Inorg. Chem.* **1992**, *31*, 145–148.
- (24) Brown, S. P.; Perez-Torralba, M.; Sanz, D.; Claramunt, R. M.; Emsley, L. *Chem. Commun.* **2002**, 1852–1853.
- (25) Lesage, A.; Emsley, L.; Chabanas, M.; Coperet, C.; Basset, J. M. *Angew. Chem. Int. Ed.* **2002**, *41*, 4535–+.
- (26) Brown, S. P.; Emsley, L. *J. Magn. Reson.* **2004**, *171*, 43–47.
- (27) Lai, W. C.; McLean, N.; Gansmüller, A.; Verhoeven, M. A.; Antoniolli, G. C.; Carravetta, M.; Duma, L.; Bovee-Geurts, P. H. M.; Johannessen, O. G.; de Groot, H. J. M.; et al. *J. Am. Chem. Soc.* **2006**, *128*, 3878–3879.
- (28) De Paepe, G.; Giraud, N.; Lesage, A.; Hodgkinson, P.; Bockmann, A.; Emsley, L. *J. Am. Chem. Soc.* **2003**, *125*, 13938–13939.
- (29) De Paepe, G.; Lesage, A.; Steuernagel, S.; Emsley, L. *ChemPhysChem* **2004**, *5*, 869–875.
- (30) Vanderhart, D. L.; Earl, W. L.; Garroway, A. N. *J. Magn. Reson.* **1981**, *44*, 361–401.
- (31) Duma, L.; Lai, W. C.; Carravetta, M.; Emsley, L.; Brown, S. P.; Levitt, M. H. *ChemPhysChem* **2004**, *5*, 815–833.
- (32) Christiansen, S. C.; Zhao, D. Y.; Janicke, M. T.; Landry, C. C.; Stucky, G. D.; Chmelka, B. F. *J. Am. Chem. Soc.* **2001**, *123*, 4519–4529.
- (33) Hedin, N.; Graf, R.; Christiansen, S. C.; Gervais, C.; Hayward, R. C.; Eckert, J.; Chmelka, B. F. *J. Am. Chem. Soc.* **2004**, *126*, 9425–9432.
- (34) Fung, B. M.; Khitrin, A. K.; Ermolaev, K. *J. Magn. Reson.* **2000**, *142*, 97–101.
- (35) Bauer, C.; Freeman, R.; Frenkiel, T.; Keeler, J.; Shaka, A. J. *J. Magn. Reson.* **1984**, *58*, 442–457.
- (36) Baldus, M.; Geurts, D. G.; Hediger, S.; Meier, B. H. *J. Magn. Reson. Ser. A* **1996**, *118*, 140–144.
- (37) Geen, H.; Freeman, R. *J. Magn. Reson.* **1991**, *93*, 93–141.
- (38) Bak, M.; Rasmussen, J. T.; Nielsen, N. C. *J. Magn. Reson.* **2000**, *147*, 296–330.
- (39) Hodgkinson, P.; Emsley, L. *Prog. Nucl. Magn. Reson. Spectrosc.* **2000**, *36*, 201–239.
- (40) Bak, M.; Nielsen, N. C. *J. Magn. Reson.* **1997**, *125*, 132–139.
- (41) Tomlinso, Bl.; Hill, H. D. W. *J. Chem. Phys.* **1973**, *59*, 1775–1784.
- (42) Emsley, L.; Burghardt, I.; Bodenhausen, G. *J. Magn. Reson.* **1990**, *90*, 214–220.
- (43) Freeman, R. *Chem. Rev.* **1991**, *91*, 1397–1412.
- (44) Vold, R. L.; Vold, R. R. *Prog. Nucl. Magn. Reson. Spectrosc.* **1978**, *12*, 79–133.
- (45) Miao, X. J.; Freeman, R. *J. Magn. Reson. Ser. A* **1996**, *119*, 90–100.
- (46) Kupce, E.; Boyd, J.; Campbell, I. D. *J. Magn. Reson. Ser. B* **1995**, *106*, 300–303.
- (47) Emsley, L.; Bodenhausen, G. *J. Magn. Reson.* **1992**, *97*, 135–148.
- (48) Raleigh, D. P.; Levitt, M. H.; Griffin, R. G. *Chem. Phys. Lett.* **1988**, *146*, 71–76.
- (49) Nakai, T.; McDowell, C. A. *Mol. Phys.* **1996**, *88*, 1263–1275.
- (50) Ottiger, M.; Delaglio, F.; Bax, A. *J. Magn. Reson.* **1998**, *131*, 373–378.
- (51) Andersson, P.; Weigelt, J.; Otting, G. *J. Biomol. NMR* **1998**, *12*, 435–441.
- (52) Duma, L.; Hediger, S.; Lesage, A.; Emsley, L. *J. Magn. Reson.* **2003**, *164*, 187–195.
- (53) Duma, L.; Hediger, S.; Brutscher, B.; Bockmann, A.; Emsley, L. *J. Am. Chem. Soc.* **2003**, *125*, 11816–11817.
- (54) Bermel, W.; Bertini, I.; Duma, L.; Felli, I. C.; Emsley, L.; Pierattelli, R.; Vasos, P. R. *Angew. Chem., Int. Ed.* **2005**, *44*, 3089–3092.
- (55) Abragam, A. *Principles of Nuclear Magnetism*; Oxford University Press: New York, 1961.
- (56) Ramamoorthy, A.; Fujiwara, T.; Nagayama, K. *J. Magn. Reson. Ser. A* **1993**, *104*, 366–368.
- (57) Case, D. A.; Dyson, H. J.; Wright, P. E. *Methods Enzymol.* **1992**, *239*, 392–416.
- (58) Contreras, R. H.; Peralta, J. E.; Giribet, C. G.; De Azua, M. C.; Facelli, J. C. *Annu. Rep. NMR Spectrosc.* **2000**, *41*, 55–184.
- (59) Harris, R. K.; Knight, C. T. G. *J. Chem. Soc., Faraday Trans.* **1983**, *79*, 1539–1561.
- (60) Marsmann, H. C. *Encyclopaedia of NMR*; Grant, D. M., Harris, R. K., Eds.; Wiley: London, 1997; Vol. 7, pp 4386–4398.
- (61) Harris, R. K.; Knight, C. T. G. *J. Chem. Soc., Faraday Trans.* **1983**, *79*, 1525–1538.
- (62) Harris, R. K.; Oconnor, M. J.; Curzon, E. H.; Howarth, O. W. *J. Magn. Reson.* **1984**, *57*, 115–122.
- (63) Knight, C. T. G.; Kirkpatrick, R. J.; Oldfield, E. *J. Am. Chem. Soc.* **1986**, *108*, 30–33.
- (64) Knight, C. T. G.; Kirkpatrick, R. J.; Oldfield, E. *J. Am. Chem. Soc.* **1987**, *109*, 1632–1635.
- (65) Harris, R. K.; Parkinson, J.; SamadiMaybodi, A. *J. Chem. Soc., Dalton Trans.* **1997**, 2533–2534.
- (66) Kinrade, S. D.; Donovan, J. C. H.; Schach, A. S.; Knight, C. T. G. *J. Chem. Soc., Dalton Trans.* **2002**, 1250–1252.
- (67) Haouas, M.; Taulelle, F. *J. Phys. Chem. B* **2006**, *110*, 3007–3014.
- (68) Cho, H.; Felmy, A. R.; Craciun, R.; Keenum, J. P.; Shah, N.; Dixon, D. A. *J. Am. Chem. Soc.* **2006**, *128*, 2324–2335.
- (69) Helgaker, T.; Jaszunski, M.; Ruud, K. *Chem. Rev.* **1999**, *99*, 293–352.
- (70) Vaara, J.; Jokisaari, J.; Wasylishen, R. E.; Bryce, D. L. *Prog. Nucl. Magn. Reson. Spectrosc.* **2002**, *41*, 233–304.
- (71) Duma, L.; Hediger, S.; Lesage, A.; Sakellariou, D.; Emsley, L. *J. Magn. Reson.* **2003**, *162*, 90–101.